MODELLING AND ANALYSIS OF AXIAL LOADED WIRE ROPE STRAND USING THE FINITE ELEMENT METHOD

C. Erdem Imrak, Ozgur Senturk
ITU, Faculty of Mech. Eng., Mech.Eng. Department
Gumussuyu, 34437 Istanbul, Turkey

ABSTRACT
Spiral wire rope strands and overhead electrical conductors are examples of helical wire assemblies. The use of these helically wound wires constitute a wide class of important engineering components. When they are subjected to axial loads (tensile and torsional), these structures may still exhibit the helically symmetric characteristic after loading. For this reason, this feature can be used to simplify the analysis of these structures and to reduce model size in numerical simulations. In this paper, the formulation of helically symmetric boundary conditions is used and a general strand model using the finite element method (FEM) is presented. The model is capable of taking into account the effects of tension, shear, torsion, contact, friction and possible local plastic yielding and has been successfully used to predict the global behavior of simple straight wire rope strand as well as the stress distribution, which are very difficult to predict analytically. As most of the strand models, the length of the strand is assumed sufficiently long for the clamping conditions to be negligible. The finite analysis results showed excellent agreement with the analytical theory of Costello and the experimental results obtained by Utting and Jones [6, 7].
Keywords: wire rope, strand, helical symmetry, constraint equation, finite element model

1. INTRODUCTION

Steel wire ropes are critical load-bearing components in a wide range of applications such as cranes, lifts, mine haulage, etc. A wire rope is a complex component usually consisting of six or more strands in helical form around a core made of fiber or a core which itself is a small wire rope of different construction. Each strand consists of a number of wires laid in helical form around a strand core which may be a single wire or a group of wires. Wire strands and ropes are most commonly used in applications that require a combination of tensile loading and relatively low bending rigidity, such as in lifting devices like cranes. There are many parameters which can predict the effects of possible variations of these parameters on the performance of the strand. The influence of more complicated factors such as plasticity, contact stress and friction etc. on the behavior of ropes is very difficult to predict analytically. Typical tensile loading of wire strands, cords, and ropes has been studied by many researchers. There are many of published studies on stress analysis, life prediction for wire ropes [1-7]. It has been noted however that these factors may have strong influence on the mechanism of rope failure [1, 2]. Therefore, there is requirement for a general and accurate strand model which is capable of taking into account the complicating factors noted above.

2. EXTRACTION OF MODEL

The configuration of the simple straight strand analyzed in this paper is shown in Fig. 1. The strand consists of a straight circular centre wire and *m* helical wires *(m = 6 in this study)*. Tension, shear, bending and twist deformations develop simultaneously together with local contact deformation when the strand is subjected to an axial load [3]. If a structure and its load exhibit some form of symmetrical and/or repetitive nature, then the analysis can be reduced to model a representative sector of it, called a "basic sector". A basic sector must have "matching edges", which means that there exists corresponding nodes on each edge, geometrically rotated by a sector angle and/or offset by a

repetitive length. By analyzing a properly selected basic sector, the responses of the complete structure can be obtained. Taking advantage of the helical symmetry of a strand, a slice of 1/12 of a 7-wire strand can be chosen as the basic sector [4].
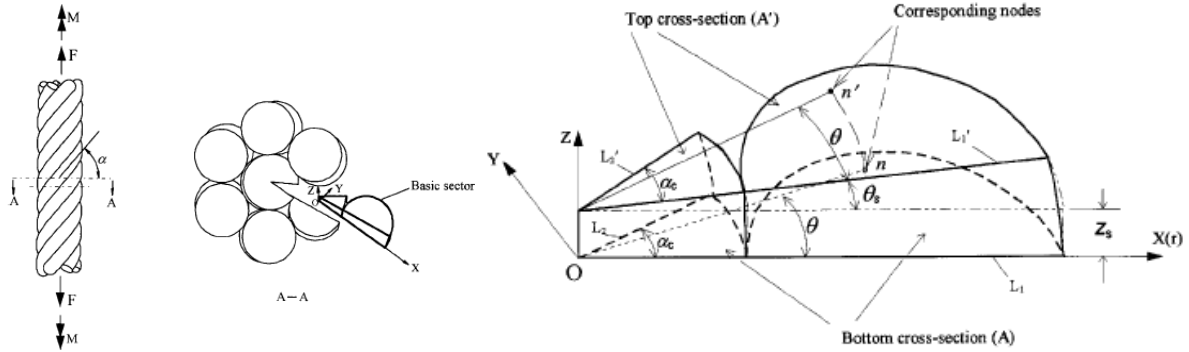

Figure 1. Simple 7-wire rope strand and geometric model of basic sector

Figure 2 shows a typical finite element mesh of the model. Figure 3 provides a more detailed view in the vicinity of local contact area. Since the stresses vary rapidly in this area, a much finer mesh was used. A commercial finite element analysis software (ANSYS) was used throughout [2]. Three-dimensional solid brick elements were used for structural discretization. This element is defined by eight nodes having three degrees of freedom on each, i.e. translations in *x, y* and z directions. Only one element division is needed in the strand axial direction to consider the helical effect, due to the accurate boundary conditions, as will be discussed in the following section. Contacts between the centre and helical wires have been simulated using contact elements between the surfaces. They can simulate general surface-to-surface contact with Coulomb friction sliding. Precise boundary conditions are maintained by using the constraints equations which relate the displacements of the corresponding nodes on the top and bottom cross-sections of the strand.
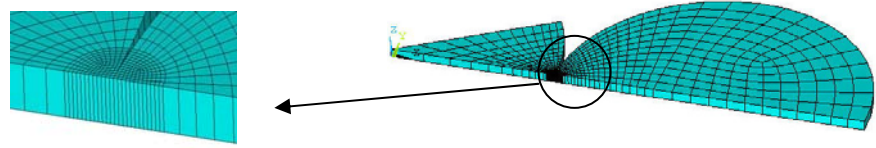

Figure 2. Finite element mesh of rope basic sector

3. FORMULATION OF CONSTRAINT EQUATIONS

Constraint equations define the relationships between a set of degrees of freedom within the model mesh. The strand extension due to an applied axial strain ε, the twist angle of the strand due to an applied twist rate Γ and the helical rotation angle between the top and bottom cross-sections can be defined as follows

$$\delta z_s = \varepsilon z_s \quad , \quad \delta\theta_s = \Gamma z_s \quad , \quad \theta_s = 2\pi z_s / p . \tag{1}$$

For general helical symmetry (see Fig. 3), constraint equations between the displacements of the corresponding nodes $n(r, \theta, z)$ and $n'(r, \theta+\theta_s, z+z_s)$ can be expressed as

$$\mathbf{u}' = \mathbf{R}\mathbf{u} + \mathbf{u}_\Gamma + \mathbf{u}_\varepsilon \tag{2}$$

where $\mathbf{u} = (u_x, u_y, u_z)^T$ is the displacement vector of node n, $\mathbf{u}' = (u_x', u_y', u_z')^T$ is the displacement vector of the corresponding node n' and $\mathbf{u}_\Gamma = (\,-2r\sin(\delta\theta/2)\sin(\theta + \theta_s + (\delta\theta/2)), \, 2r\sin(\delta\theta/2)\cos(\theta + \theta_s + (\delta\theta/2)), \, 0)^T$ is the relative rotational displacement vector, $\mathbf{u}_\varepsilon = (0, 0, \delta z_s)^T$ is the relative extension displacement vector and $\mathbf{R}$ the rotational matrix

$$\mathbf{R} = \begin{bmatrix} \cos(\theta_s + \delta\theta_s) & -\sin(\theta_s + \delta\theta_s) & 0 \\ \sin(\theta_s + \delta\theta_s) & \cos(\theta_s + \delta\theta_s) & 0 \\ 0 & 0 & 1 \end{bmatrix} \tag{3}$$

The four radial edge lines L_1, L_1', L_2 and L_2' shown in Figure 2 are initially straight and perpendicular to the strand axis. They should remain straight and perpendicular to the strand axis after deformation. The sector angle of *180°/m* (30° for a 7-wire strand) will remain unchanged on both top and bottom cross-sections.
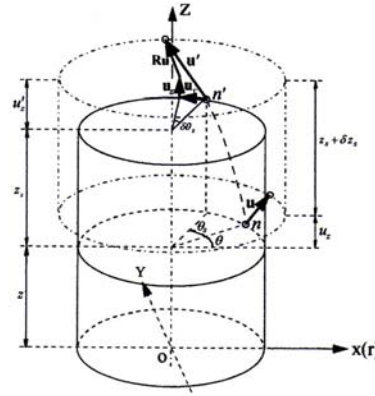
Figure 3. Helical symmetric constraint relationship

Consider now a pair of corresponding nodes on the corresponding radial lines; on the one hand they are on helically symmetric boundaries, hence should obey the helical symmetric relationship; on the other, they are on the four radial edge lines, therefore they should obey the straight line deformation relationship as well. Degree of freedom constraints to eliminate rigid-body movement were also introduced on these nodes.

$$u_y = 0 \ , \ u_z = 0$$

For (L$_1$, L$_1$'):

$$u'_x = \cos(\theta_s + \delta\theta_s) \, u_x - 2r\sin(\delta\theta_s / 2)\sin(\theta_s + (\delta\theta_s / 2))$$

$$u'_y = \sin(\theta_s + \delta\theta_s) \, u_x + 2r\sin(\delta\theta_s / 2)\cos(\theta_s + (\delta\theta_s / 2))$$

$$u'_z = \delta \, z_s$$

(4)

$$u_y = \tan\alpha_c.u_x \ , \ u_z = 0$$

For (L$_2$, L$_2$'):

$$\begin{pmatrix} u'_x \\ u'_y \end{pmatrix} = \begin{bmatrix} \cos(\theta_s + \delta\theta_s) & -\sin(\theta_s + \delta\theta_s) \\ \sin(\theta_s + \delta\theta_s) & \cos(\theta_s + \delta\theta_s) \end{bmatrix} \begin{pmatrix} u_x \\ \tan\alpha_c.u_x \end{pmatrix}$$
$$+ \begin{pmatrix} -2r\sin(\delta\theta_s / 2)\sin(\alpha_c + \theta_s + (\delta\theta_s / 2)) \\ 2r\sin(\delta\theta_s / 2)\cos(\alpha_c + \theta_s + (\delta\theta_s / 2)) \end{pmatrix}$$

(5)

$$u'_z = \delta \, z_s$$

4. FINITE ELEMENT ANALYSIS RESULTS

Responses to axial and torsional loads for a simple 7-wire strand have been analyzed using the 1/12-strand finite element model developed. The geometry data of the strand is given in Table 1. The Von Mises yield criterion was assumed. A bilinear isotropic hardening material model [2] has been used. Geometric non-linear effects were also taken into account. The basic parameters for the 1/12-strand finite element model are summarized in Table 1.

Table 1. The geometry data and parameters of the model

Strand diameter	11,4 mm	Total number of nodes	1516
Center wire diameter $2R_1$	3,94 mm	Total number of solid elements	684
Helical wire diameter $2R_2$	3,73 mm	Young's modulus E	188 GPa
Pitch length p	115 mm	Plastic modulus	24,6 GPa
Helical angle of the strand α	78,2°	Yield stress	1,54 GPa
Strand length used in the model z_s	%5 R_1	Limit stress	1,80 GPa
Friction coefficient μ	0,115	Poisson's ratio	0,3

The value for Young's modulus is lower than would be conventionally expected for steel, but is based on the experimental results of Walton [5] and Utting and Jones [6]. The value for the plastic modulus was determined from the results of Walton [4, 5] at the lower end of the plastic strain range. Two extreme load cases of fixed end (Γ = 0) and free end (M = 0) were analyzed. A strand axial strain of 0,015 was applied in increments of 0,001 in the analysis. The results have been compared to those obtained using Costello's theory [3], and the experimental data reported by Utting and Jones [7]. Figure 4a shows the

load as a function of the applied axial strain for both the fixed and free end cases. Figure 4b gives the variation of torque with load for the fixed end condition and Figure 4c shows the dependence of strand twist rate against load for the free end condition. The finite element analysis predicts the same strand responses in the linear region as given by Costello's theory and the test results obtained by Utting and Jones [6, 7]. In the non-linear region, the results from the present FE model fit the test data very well.
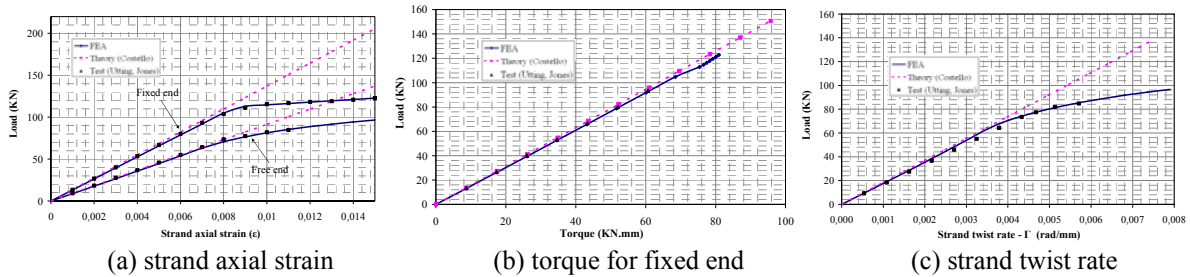

| (a) strand axial strain | (b) torque for fixed end | (c) strand twist rate |

Figure 4. Axial load distribution on wire rope

As would be expected, the ratio of peak stress: average bulk stress decreases after local yielding has occurred. Figure 5 shows the axial stress σ_z distribution along the same radial line. With the same strand axial strain, the helical wires with a free end condition carry less axial load than with a fixed end. This is the reason that the axial (tensile) rigidity with the free end condition is less than that with a fixed end.
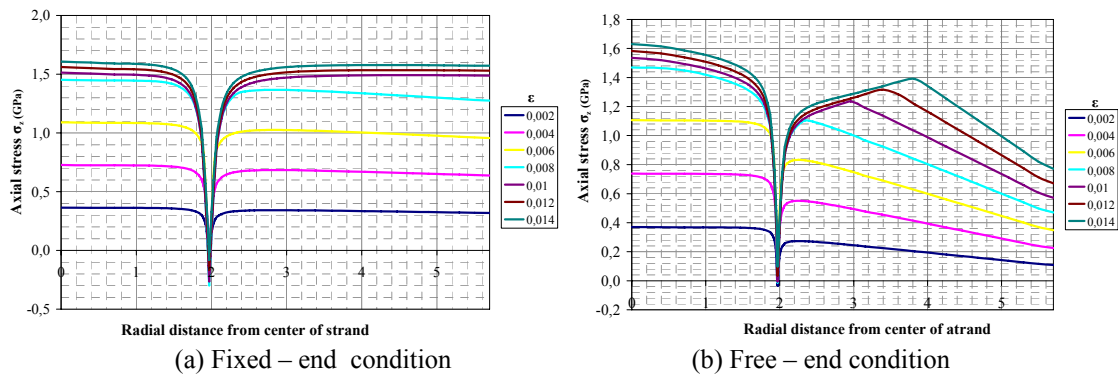

| (a) Fixed – end condition | (b) Free – end condition |

Figure 5. Stress distribution, σ_z along a radial line

5. CONCLUSION

In the implementation of the finite element analysis in this study, accurate boundary conditions were established and hence more accurate results obtained. By comparison with elasticity theory of Costello and experimental data obtained by Utting and Jones, the finite element model developed in this study has shown excellent agreement in the determination of the global responses of a rope strand. Furthermore, this model can provide information about non-linear effects, such as contact stresses, friction and plastic deformation which are very difficult to address theoretically, but play important roles in the failure mechanism of wire strand and rope.

6. REFERENCES

[1] İmrak, C.E, Gerdemeli, I.: Modeling and Stress Analysis of Axial Loaded Wire Ropes, V. Int. Congress on MET'06, Vol 4, Varna, Bulgaria, 2006.
[2] Sentürk, O.: Modeling and Analysis of Axial Loaded Wire Rope Strand Using the Finite Element Method, MSc Thesis, ITU. Inst. Sci. & Tech., Istanbul, Turkey, 2007. (in Turkish)
[3] Costello, G.A.: Theory of Wire Ropes, Springer, Berlin, 1995.
[4] Jiang, W.G., Henshall, J.L., Walton, J.M.: Concise finite element model for three-layered straight wire rope strand, Int J of Mech Sci, 42(1), 63-85, 2000.
[5] Walton, J.M.: Developments in steel cables, Journal of Constructional Steel Research, 39(1), 3-29, 1996.
[6] Utting WS, Jones N. The response of wire rope strands to axial tensile loads: part I. Int J of Mech Sci 29(9), 605-619, 1987.
[7] Utting W.S, Jones N.: The response of wire rope strands to axial tensile loads: part II. Int J of Mech Sci 29(9), 621-636, 1987.